Processing and Application of Ceramics 14 [3] (2020) 242–250
https://doi.org/10.2298/PAC2003242S



# Processing of lanthanum doped $CaCu_3Ti_4O_{12}$ electroceramics in molten eutectic mixture for low loss high dielectric materials

Arindam Sen*

*Department of Electronics, Bankura Christian College, Bankura-722101, West Bengal, India*

Received 22 May 2020; Received in revised form 1 July 2020; Accepted 18 July 2020

## Abstract

*Giant dielectric material $CaCu_3Ti_4O_{12}$ (CCTO) has found widespread applications, but associated high dielectric loss is still a major concern. The decreasing of dielectric tangent loss ($\tan\delta$) via rare earth element doping has been proven to be effective strategy, but in most cases it involves complex and time consuming processing. In the present paper, a fast and facile process is reported for the synthesis of lanthanum doped CCTO powders ($Ca_{1-x}La_xCu_3Ti_4O_{12}$ where x = 0.0, 0.05 and 0.1) using molten eutectic mixture as the reaction medium. The obtained powders were pressed and finally sintered at 1050 °C. $La^{3+}$ substitution at $Ca^{2+}$ site results in remarkable reduction in dielectric loss ($\tan\delta < 0.03$) at room temperature compared to the parent CCTO. The increased grain boundary resistance ($R_{gb}$) estimated from room temperature complex impedance plane plot ($Z^*$) for the doped ceramics is proposed to be the major cause for higher thermal stability of dielectric constant ($\varepsilon_r$) and remarkable reduction in $\tan\delta$ at room temperature. Furthermore, the frequency and temperature stability of $\varepsilon_r$ and $\tan\delta$ over wide ranges make the doped CCTO a promising candidate for high temperature ceramic capacitor application.*

***Keywords:*** *$CaCu_3Ti_4O_{12}$ ceramics, dielectric properties, microstructure, perovskites, sintering*

## I. Introduction

Materials having high dielectric constant serve as the key to realize high performance miniaturized microelectronic and memory devices. Advent of electroceramic compounds like $CaCu_3Ti_4O_{12}$ (CCTO) [1,2] with giant dielectric constant is a big boost in this field as it can allow miniaturization of capacitive components, thereby shrinking the size of electronic devices. The stunning dielectric features of this toxic free compound has already been tested for applications like multi-layer ceramic capacitors (MLCC) [3], microwave devices and antennas [4], gas and humidity sensor [5,6], supercapacitor [7,8] etc. Despite the advantage of unusually high dielectric constant ($\varepsilon_r \sim 10^4$–$10^5$) of CCTO, a member of $ACu_3Ti_4O_{12}$ family having body centred cubic perovskite structure, it is always associated with considerably high dielectric tangent loss ($\tan\delta > 0.05$ at 1 kHz at room temperature) together with low breakdown voltage, which cast a shadow on its application in capacitor. High $\tan\delta$ of a dielectric can essentially lead to self-discharging of capacitor and irreversible energy loss in high frequency applications. Thus, dedicated research efforts should be paid to lower the dielectric tangent loss even with partial sacrifice of dielectric constant which is already too high.

Different strategies have been adopted so far to obtain low loss CCTO such as: elemental substitution, improved synthesis route, controlling of microstructure and intrinsic properties of grain boundaries. Out of all these strategies, substitution of different single/multiple elements into Ca, Cu, Ti and O sites [9–15] and insulating phase doping [16–18] in CCTO crystal have been widely investigated with varied success in loss management. In particular, lanthanum doped CCTO [19–23] has shown a good success in reducing the tangent loss. For example, Feng *et al.* [19] have synthesized La-doped CCTO by conventional solid state reaction and found a considerable reduction in $\tan\delta$ in mid frequency range (2–200 kHz) with increase of doping level. Suppressed $\tan\delta$ due to La doping was also reported for samples synthesized via thermal decomposition [20], sol-gel method and citrate auto-ignition route [21] and

* Corresponding authors: tel: +91 8918444132,
e-mail: *arsen.in@gmail.com*

typical value at 10 kHz remains in the range of 0.012–0.08. In sharp contrast, La-doped CCTO synthesized by Srivastava *et al.* [24] via semi-wet route has shown increase of $\tan\delta$ with simultaneous increase of dielectric constant. Despite tremendous efforts, dielectric loss management still remains a fundamental challenge, particularly reducing the value below 0.05 (at 10 kHz) remains a formidable task. Furthermore, the frequently used method of long sintering at high temperature is highly energy consuming and thus not promising for commercial applications.

Here a facile, fast molten salt route is used for lanthanum doping in CCTO with high tunability in dielectric tangent loss. Molten salt serve as the unique medium which takes both the advantages of liquid phase processing and high temperature sintering. In the liquid medium of molten salt of eutectic mixture, crystal growth of CCTO with cube morphology and simultaneous doping with La occur. The effect of La doping via this molten salt route in CCTO on dielectric and AC conductivity properties is thoroughly studied and origin of highly suppressed tangent loss is elucidated in the present work.

## II. Experimental

In this work, $Ca_{1-x}La_xCu_3Ti_4O_{12}$ ($x$ = 0.0, 0.05, 0.1) powders were synthesized via a facile molten salt method [7]. Analytical grade $Ca(C_2H_3O_2)_2 \cdot H_2O$, $Cu(C_2H_3O_2)_2 \cdot H_2O$, $La(CH_3CO_2)_3 \cdot xH_2O$ and $TiO_2$, having purity higher than 99.95% were used as La-doped CCTO precursors while NaCl-KCl salt mixture of eutectic composition (1:1) had served as molten salt medium because of its low melting temperature (657 °C). In a typical run, the corresponding stoichiometric amounts of Ca-, La-, Cu- and Ti-precursor powders and NaCl and KCl were thoroughly mixed in a molar ratio of 1:3:4:40:40 and ground in a pestle and mortar for 1 h. High purity alumina crucible containing the mixture was then placed in a preheated (850 °C) muffle furnace and calcined at that temperature for 1 h in air. Furnace cooled samples were then washed several times with ample amount of deionized water, filtered and finally dried overnight in an oven at 80 °C prior to characterization. The process could be easily repeated to produce grams of synthesized materials. The obtained powders were pressed into pellets of ~15 mm in diameter and ~1.5 mm in thickness without any additive with the help of a hydraulic press at a pressure of 150 MPa. The pellets were finally sintered at 1050 °C for 5 h in the air to get the La-doped CCTO ceramic samples.

The densities of the sintered ceramics were determined by the Archimedes technique. The relative density was calculated on the basis of the ratio of the measured density to the theoretical density of CCTO (5.05 g/cm$^3$). Crystallographic phases of the calcined powders were identified using powder X-ray diffractometer (XRD, Bruker, D-8 Advance) employing Cu-K$\alpha$ radiation of wavelength $\lambda$ = 1.5406 Å at room temperature. Field emission scanning electron microscope (FESEM, Hitachi S4800) was used to investigate the size distribution and morphology of the calcined powders as well as sintered pellets. An energy-dispersive X-ray spectroscopy (EDS) attached to the FESEM was used for detection and estimation of elements in the prepared compound. Before measuring electrical properties, the top and bottom surfaces of the sintered pellets were polished and covered with conductive silver paint followed by firing at 200 °C for 20 min in air. A computer controlled precision LCR meter (Agilent E4980A) with an oscillating voltage of 0.5 V was used to measure dielectric properties of the sintered pellets over a broad frequency and temperature ranges of 20 Hz to 2 MHz and 30 to 200 °C, respectively.

## III. Results and discussion

### 3.1. XRD analysis

Figure 1 shows the room temperature powder X-ray diffraction patterns of $Ca_{1-x}La_xCu_3Ti_4O_{12}$ powders with different $La^{3+}$ doping concentrations. All the diffraction peaks in XRD patterns are perfectly indexed based on body centred cubic perovskite structure of CCTO (JCPDS card No 75-2188) and approve the monophasic formation of the compound up to $x$ = 0.1 La substitution

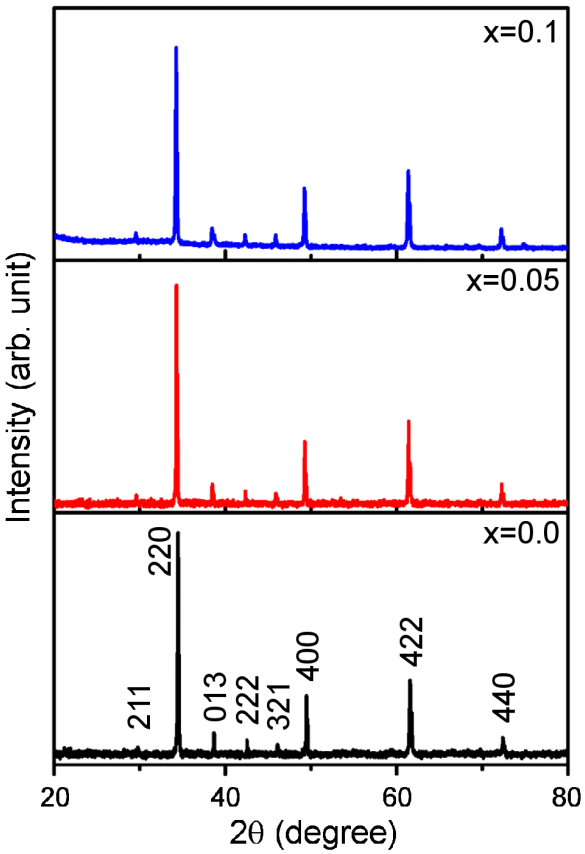


**Figure 1. X-ray diffraction patterns of $Ca_{1-x}La_xCu_3Ti_4O_{12}$ ($x$ = 0.0, 0.05, 0.1) powders synthesized at 850 °C for 1 h**

with no trace of peaks due to constituent oxides or other impurity phases. The calculated values of lattice parameter a for the $Ca_{1-x}La_xCu_3Ti_4O_{12}$ powders calcined at 850 °C for 1 h are 7.381, 7.392 and 7.401 Å for $x$ = 0.0, 0.05 and 0.1, respectively, which are comparable to the values found in the literature [20,23]. However, there is a slight increase in lattice parameter with increasing La doping, which can be attributed by the replacement of smaller $Ca^{2+}$ by larger $La^{3+}$ ions [25]. The change in lattice parameter indicates that $La^{3+}$ has substituted $Ca^{2+}$ in its lattice position in the doped ceramics without altering the crystal structure of CCTO. The XRD results indicate that the pure and La-doped CCTO powders can be successfully prepared by a facile molten salt method at a relatively low calcination temperature and short reaction time.

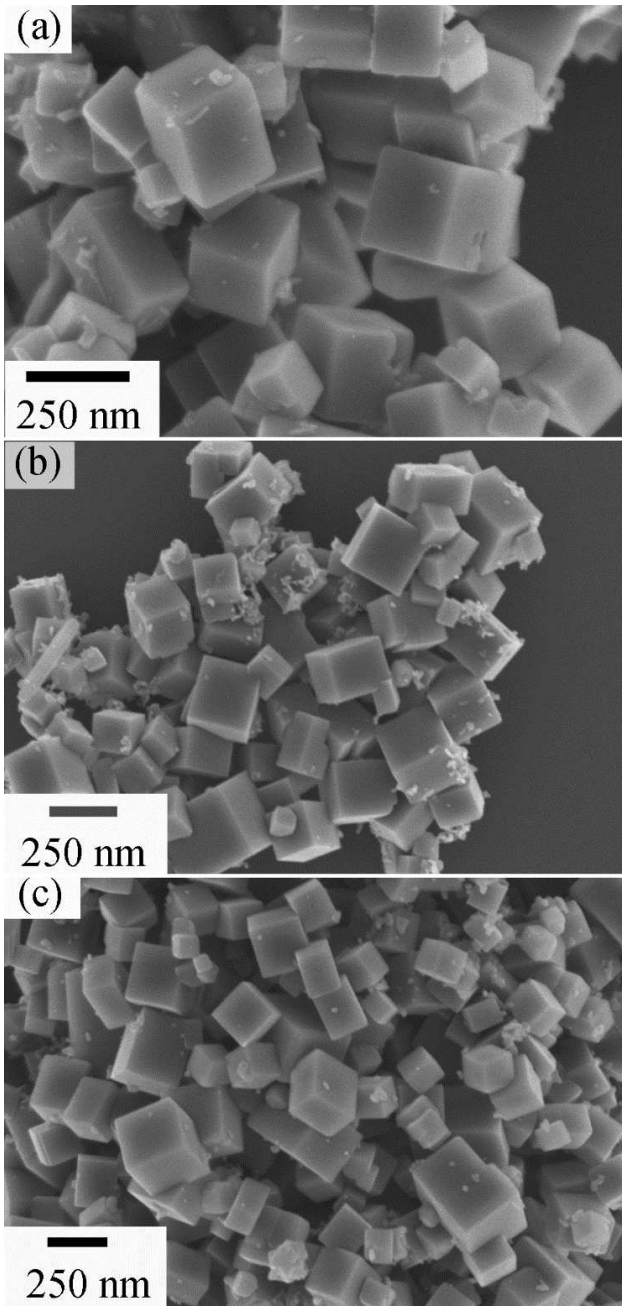


**Figure 2. FESEM images of La-doped CCTO powders synthesized at 850 °C/1 h for: a) $x$ = 0.0, b) $x$ = 0.05 and c) $x$ = 0.1**

### *3.2. Microstructure analysis*

Figure 2 displays FESEM images revealing the size and morphology of the as-prepared pure and La-doped CCTO samples synthesized at 850 °C for 1 h. Cube morphology can be observed in all the as-synthesized samples. It is clear from Fig. 2a that the as-prepared sample ($x$ = 0.0) obtained by molten salt route consists of distinct cubes with smooth faces and clear, well-defined edges having mean edge length of ~250 nm. However, cube size is found to decrease slightly with increasing La doping concentration and it becomes ~200 nm for the sample with $x$ = 0.1 (Fig. 2c). In order to confirm the chemical composition of the as-prepared cubes, EDX analysis was carried out for the as-prepared $Ca_{1-x}La_xCu_3Ti_4O_{12}$ ($x$ = 0.1) sample synthesized at 850 °C for 1 h as shown in Fig. 3. The atomic percentages of Ca, La, Cu, Ti and O are found to be 5.54%, 0.60%, 17.73%, 24.89% and 67.54%, respectively which is close to the stoichiometric ratio approving thereby the purity of the sample without any trace of impurity prepared by the molten salt route.

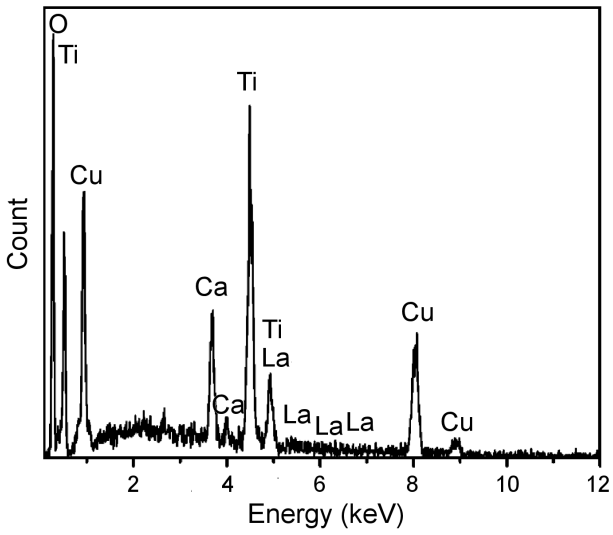


**Figure 3. EDS spectrum of $Ca_{1-x}La_xCu_3Ti_4O_{12}$ ($x$ = 0.1) powder synthesized at 850 °C for 1 h**

To investigate the role of microstructure on the electrical properties of these ceramics, the cubes synthesized by molten salt route were processed into bulk ceramics, without the addition of sintering additive. Figure 4 shows the microstructures of the fractured surface of all the ceramics sintered at 1050 °C for 5 h indicating a drastic decrease in the mean grain size with increasing La doping concentration. However, in all the ceramic samples, the grains are well-defined and can be clearly identified. Figure 4a shows bimodal grain size distribution for the pure CCTO ceramics in which small grains (~3–6 μm) are distributed among extremely large

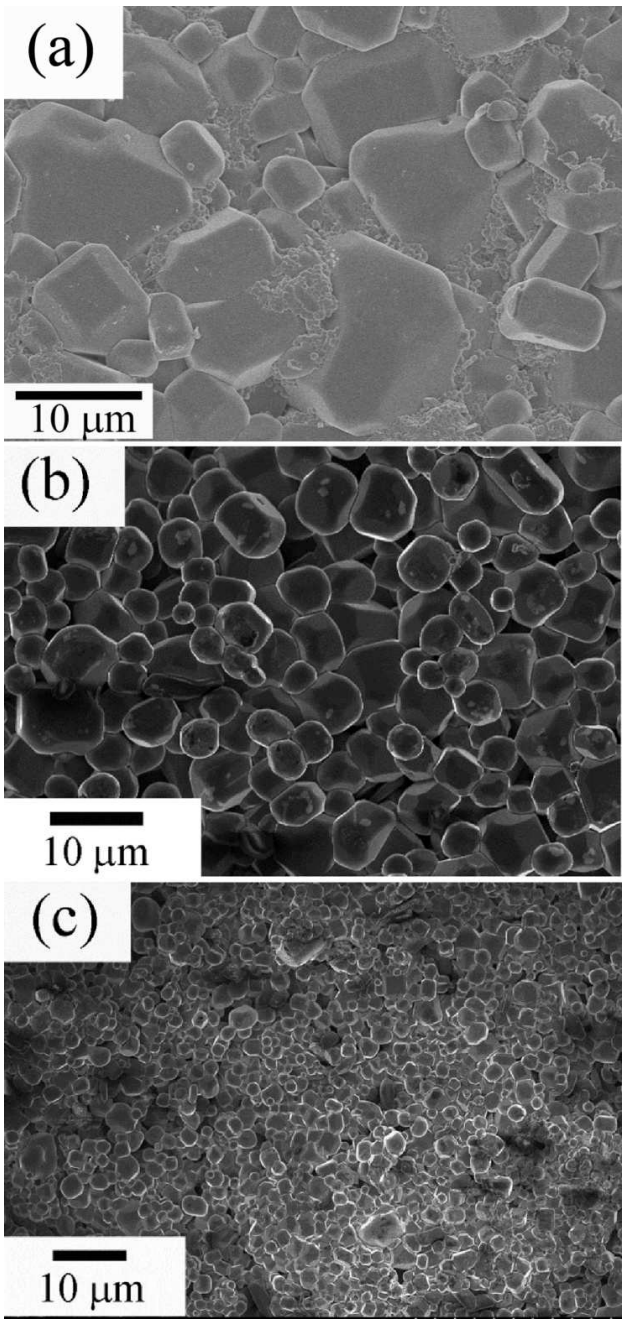


**Figure 4. FESEM images of $Ca_{1-x}La_xCu_3Ti_4O_{12}$ ceramic pellets sintered at 1050 °C for 5 h: a) $x$ = 0.0, b) $x$ = 0.05 and c) $x$ = 0.1**

grains (~15–20 μm) and mean grain size estimated from the micrograph is found to be ~9.85 μm. It is to be noted that the mean grain size of the doped ceramics ($x$ = 0.05) has been significantly reduced (~4.2 μm) and grain morphology is found to be homogeneous in size and regular in shape (Fig. 4b). This tendency of grain refinement became more obvious for the sample with higher La doping concentration ($x$ = 0.1) having grain size ~2.2 μm (Fig. 4c) and increased portion of porosity. The densities of the La-doped CCTO ceramics are estimated to be 4.85, 4.74, and 4.59 g/cm$^3$ corresponding to 96.03%, 93.86% and 90.89% of theoretical density for $x$ = 0.0, 0.05 and 0.1, respectively. The density values depict that the ceramics with $x$ = 0.1 has lower density demonstrating that the La doping could be beneficial when the doping level is not very high. The decrease in the mean grain size of the La-doped CCTO ceramics is well supported by other researchers and may be credited to the influence of $La^{3+}$ doping ions suppressing grain boundary mobility during sintering. These observations clearly indicate that La substitution for Ca site has effectively prohibited the growth of large grains and at the same time reduced the mean grain size of CCTO ceramics. The observed microstructural disparity of these samples is adequate to cause the variation in their dielectric properties.

### *3.3. Dielectric properties of sintered pellets*

The influence of La substitution on dielectric constant ($\varepsilon_r$) and dielectric loss ($\tan\delta$) of the CCTO ceramics sintered at 1050 °C for 5 h is evident from their plots of frequency variation at room temperature (Fig. 5). A monotonic decrease in the value of $\varepsilon_r$ is observed for all the ceramics in the low frequency range (< 100 Hz) as is evident from Fig. 5a. The high $\varepsilon_r$ for all the ceramics at low frequency is due to interfacial space charge polarization and electrode effect [26], which arises due to microstructural inhomogeneity. $\varepsilon_r$ of the pure CCTO shows decrease in value with increase in measured frequency whereas $\varepsilon_r$ of the La-doped CCTO exhibits weak frequency dependence especially in the frequency range between 1–500 kHz. In addition, the ceramics with $x$ = 0.05 exhibits slightly broader $\varepsilon_r$ plateau with feeble frequency dependence compared to other samples and the well-known Debye-type relaxation at high frequency is also not observed because of the limit of measured frequency range. However, the relaxation frequency is shifted to lower frequency side (~500 kHz) with increasing doping concentration ($x$ = 0.1). It is observed that the values of $\varepsilon_r$, at 10 kHz and at 30 °C, are 5244, 2233 and 1719 for the $Ca_{1-x}La_xCu_3Ti_4O_{12}$ ceramics with $x$ = 0.0, $x$ = 0.05 and $x$ = 0.1, respectively. This confirms that $\varepsilon_r$ decreases 2.35 and 3.05 times with increasing La doping in comparison to the pure CCTO. This decline can be correlated to microstructural dissimilarity, mainly to the grain sizes. Similar dielectric behaviour has already been reported in the literature for pure and La-doped CCTO ceramics [19,21]. These observations facilitate to conclude that microstructure as well as dielectric properties are significantly influenced by La substitution at Ca site of CCTO.

Frequency dependence of $\tan\delta$ at room temperature (Fig. 5b) of the pure and La-doped CCTO ceramics depicts that $\tan\delta$ is decreased at first at low frequency (<1 kHz), remains invariant over a wide frequency range followed by an increasing trend above $10^5$ Hz. The $\tan\delta$ for the doped ceramics is higher at low frequencies up to 2 kHz and remains lower (<0.05) than that of the pure CCTO from 2 to 100 kHz and thereafter displays a slowly growing trend. DC conduction processes [27] are usually associated with the rise in $\tan\delta$ at low frequencies while increase in $\tan\delta$ at high frequencies can be

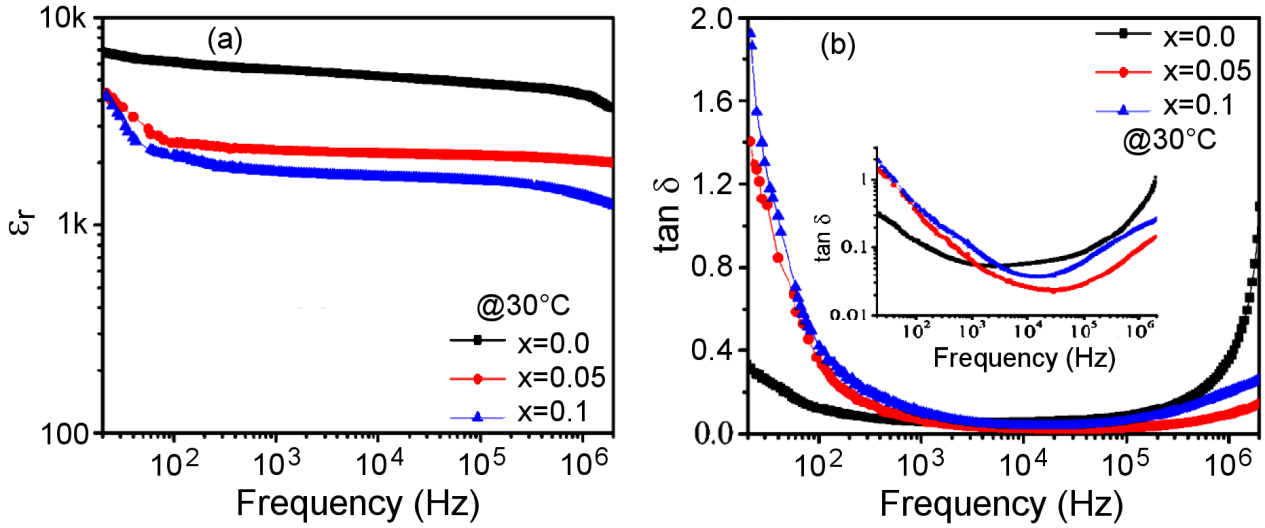


**Figure 5. Frequency dependence of: a) dielectric constant ($\varepsilon_r$) and b) dielectric loss (tan $\delta$) at room temperature of $Ca_{1-x}La_xCu_3Ti_4O_{12}$ ($x$ = 0.0, 0.05, 0.1) ceramics**

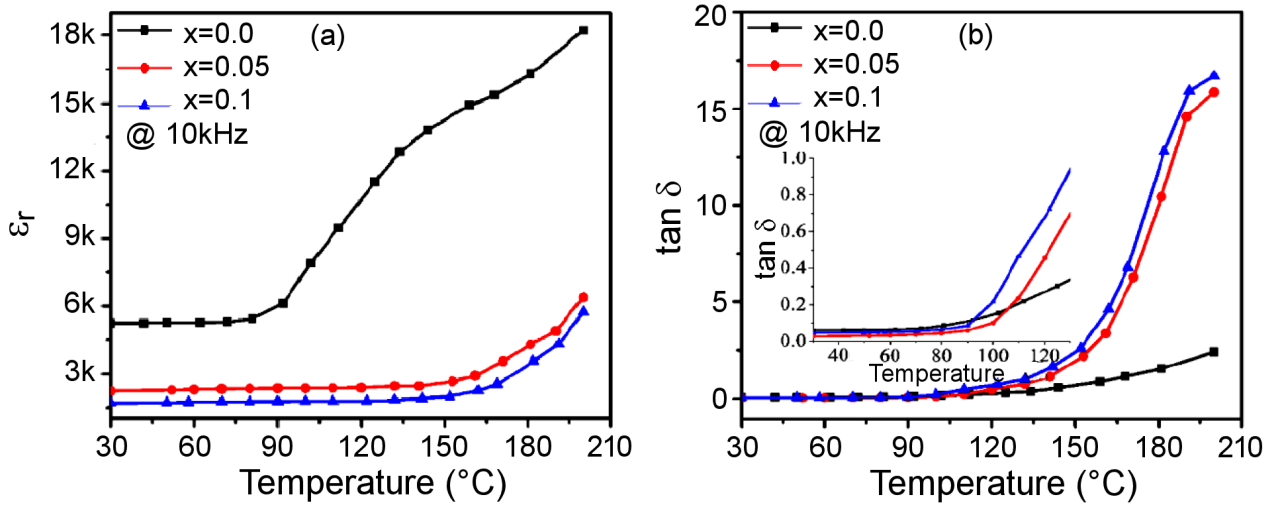


**Figure 6. Temperature dependence of: a) dielectric constant ($\varepsilon_r$) and b) dielectric loss (tan $\delta$) at 10 kHz of $Ca_{1-x}La_xCu_3Ti_4O_{12}$ ($x$ = 0.0, 0.05, 0.1) ceramics**

correlated with dielectric relaxation process [28]. The values of tan $\delta$ at room temperature and at 10 kHz are 0.059, 0.026 and 0.038 while minimum tan $\delta$ values of 0.054, 0.022, 0.032 are obtained at 2.5, 29 and 12 kHz for the ceramics with $x$ = 0.0, $x$ = 0.05 and $x$ = 0.1, respectively. In addition, Fig. 5b also clearly indicates that tan $\delta$ of the pure CCTO is greater than 0.05 over the entire measured frequency range whereas tan $\delta$ values for the doped ceramics ($x$ = 0.05) are lower than 0.03 over a wide frequency range (2–120 kHz). Also, the doped ceramics ($x$ = 0.05) exhibits lower tan $\delta$ values than that of all other samples at the frequency ranging from 1.2 kHz to 1 MHz as can be clearly seen in the inset of Fig. 5b. Based on the above results, it can be concluded that the La-doped CCTO ceramics exhibits reasonably stable $\varepsilon_r$ and very low tan $\delta$ values over a wide frequency range at room temperature which is beneficial for capacitor application.

Figure 6 shows the variation of $\varepsilon_r$ and tan $\delta$ with temperature at 10 kHz for the CCTO ceramics with different La concentrations. The $\varepsilon_r$ and tan $\delta$ values at 30 °C and 10 kHz of all the ceramics along with temperature stability of $\varepsilon_r$ are shown in Table 1. Temperature stability of dielectric constant ($\Delta\varepsilon_r$) is calculated by the following equation:

$$\Delta\varepsilon_r = \frac{\varepsilon_T - \varepsilon_{30\,^\circ\mathrm{C}}}{\varepsilon_{30\,^\circ\mathrm{C}}} \cdot 100 \qquad (1)$$

where $\varepsilon_T$ and $\varepsilon_{30\,^\circ\mathrm{C}}$ are $\varepsilon_r$ at a temperature of $T$ and 30 °C, respectively. It is evident from Table 1 and Fig. 6a that temperature stability of $\varepsilon_r$ for the doped samples is better than that of the pure CCTO. All the doped ceramics exhibit negligible variation in $\varepsilon_r$ with temperature ($\Delta\varepsilon_r$ < 15%) at 10 kHz in the temperature range of 30–140 °C while the undoped CCTO displays temperature independent $\varepsilon_r$ ($\Delta\varepsilon_r$ < 15%) only up to 85 °C and thereafter increases with increasing temperature showing an anomaly at around 140 °C.

**Table 1. Dielectric properties ($\varepsilon_r$ and $\tan\delta$ at 30 °C and 10 kHz) and temperature stability of $\varepsilon_r$ ($\Delta\varepsilon_r$) for $Ca_{1-x}La_xCu_3Ti_4O_{12}$ ceramics sintered at 1050 °C for 5 h**

| Sample | $\varepsilon_r$ | $\tan\delta$ | $\Delta\varepsilon_r$ | | | | |
|---|---|---|---|---|---|---|---|
| | | | 60 °C | 90 °C | 120 °C | 135 °C | 150 °C |
| $CaCu_3Ti_4O_{12}$ | 5244 | 0.059 | 0.42 | 16.74 | 119.24 | 144.83 | 164.48 |
| $Ca_{0.95}La_{0.05}Cu_3Ti_4O_{12}$ | 2233 | 0.026 | 2.86 | 5.46 | 6.40 | 9.71 | 19.21 |
| $Ca_{0.9}La_{0.1}Cu_3Ti_4O_{12}$ | 1719 | 0.045 | 1.57 | 3.14 | 4.42 | 6.92 | 16.75 |

It is observed from Fig. 6b that the $\tan\delta$ of the doped samples is temperature invariant from room temperature to 90 °C (as shown in inset) and less than that of the pure CCTO followed by sharp increase with increasing temperature. This is due to the increase in conductivity with increase in temperature as it is evident from the conductivity analysis discussed later. However, variation of $\tan\delta$ for the doped ceramics is higher than that of the undoped sample at higher temperature (>120 °C) which may be ascribed to the enhanced mobility of charge carriers due to vacancies or defects in the compound. Thus, it can be concluded that temperature and frequency stability of $\varepsilon_r$ and $\tan\delta$ for the pure CCTO ceramics can be improved by appropriate $La^{3+}$ substitution into $Ca^{2+}$ site.

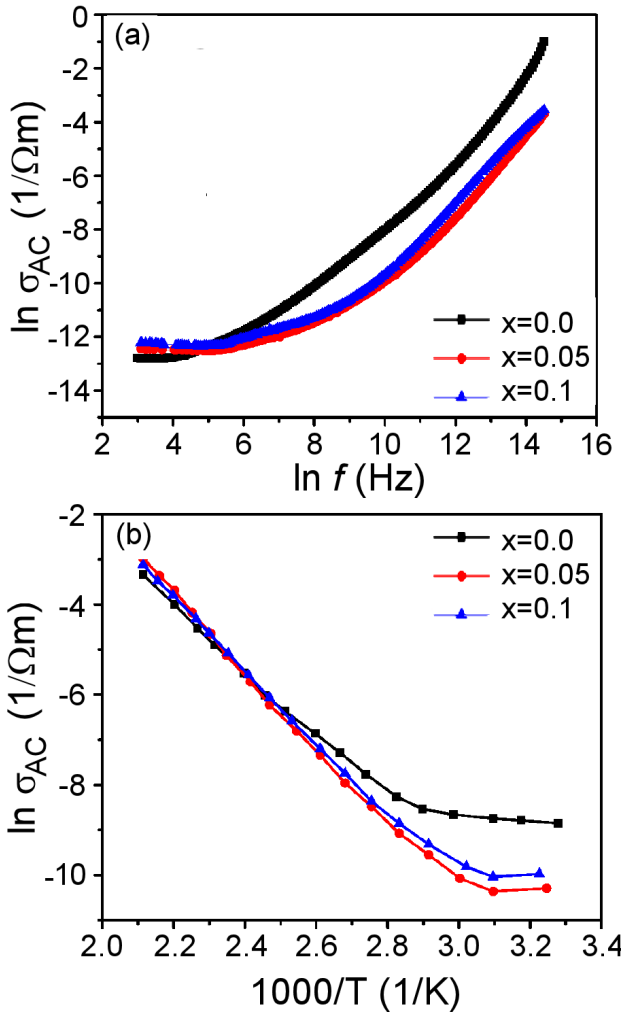


**Figure 7. Frequency dependence of AC conductivity of $Ca_{1-x}La_xCu_3Ti_4O_{12}$ ($x$ = 0.0, 0.05, 0.1) ceramics at room temperature (a) and temperature dependence of AC conductivity of $Ca_{1-x}La_xCu_3Ti_4O_{12}$ ($x$ = 0.0, 0.05, 0.1) pellets at 10 kHz (b)**

### 3.4. AC conductivity study

To gain information regarding the mechanism of conduction for the pure and La-doped CCTO ceramics, AC conductivity ($\sigma_{AC}$) is measured at room temperature as a function of frequency (Fig. 7a). The curves reveal that conductivity of all the ceramics synthesized by molten salt route increases with frequency in general but decreases with increase in La substitution. In addition, low frequency plateau region which corresponds to DC conductivity is slightly greater for the doped ceramics than that of the undoped one and it is responsible for their increased dielectric loss in the low frequency region. With $x = 0.05$, the conductivity decreases abruptly from that of the pure CCTO. Although the doped ceramics exhibits almost identical conductivity dispersion, conductivity increases slightly with more La incorporation ($x = 0.1$). This is in agreement with the dielectric loss behaviour found in the doped ceramics as shown in Fig. 5b.

Figure 7b shows the variation of $\ln\sigma_{AC}$ versus $10^3/T$ at 10 kHz for the pure and La-doped CCTO ceramics. The conductivity increases with increasing temperature exhibiting a negative temperature co-efficient of resistance (NTCR) behaviour for all the ceramics. In addition, a decreasing trend in $\sigma_{AC}$ with increasing La concentration is also observed in the measured temperature range. It is also evident from Fig. 7b that La doping has significantly changed the conductivity making doped ceramics more resistive than undoped one. In addition, the temperature-dependent AC conductivity of all the ceramics displays an Arrhenius behaviour [29] which can be expressed by the following equation:

$$\sigma_{AC} = \sigma_0 \cdot \exp\frac{-E_a}{k_B \cdot T} \tag{2}$$

where $\sigma_0$, $T$, $E_a$ and $k_B$ are the pre-exponential factor, absolute temperature, activation energy and the Boltzmann's constant, respectively. The calculated activation energy ($E_a$) of the conduction obtained from the slopes of the $\ln\sigma_{AC}$ versus $10^3/T$ curve at 10 kHz are 0.57, 0.72 and 0.68 eV in the temperature range (340–480 K) for $x = 0.0$, $x = 0.05$ and $x = 0.1$ ceramics, respectively. It is to be noted that activation energy ($E_a$) values of the doped ceramics is greater than that of pure CCTO and it is consistent with the increase of their grain boundary resistance ($R_{gb}$) values as discussed below.

### 3.5. Complex impedance study

The complex impedance spectroscopy (IS) is a non-destructive technique frequently used to examine electrical responses and to correlate the microstructure to the dielectric properties of the material. This technique allows to extract useful information such as the relaxation phenomenon, conduction mechanism, as well as contribution of grain, grain boundaries and electrode-sample contact effect existing in the material. Complex impedance plane plot ($Z^*$ plots) and its high frequency tails close to the origin for the pure and La-doped CCTO samples at room temperature are shown in Fig. 8 and inset, respectively. The high and low frequency tails of complex impedance plot with non-zero intercept on $Z'$ axis on extrapolation gives grain ($R_g$) and grain boundary ($R_{gb}$) resistance values, respectively [30,31]. The $R_g$ values are found to be ~29.57, 247.38 and 325.74 Ω whereas $R_{gb}$ values are estimated to be ~$5.03 \times 10^6$, $78.1 \times 10^6$ and $57.5 \times 10^6$ Ω for the $Ca_{1-x}La_xCu_3Ti_4O_{12}$ ceramics with $x = 0.0$, 0.05 and 0.1, respectively. These results clearly indicate that $La^{3+}$ doping has strongly increased $R_{gb}$ values, which is possibly due to the ability of $La^{3+}$ doping ions to prevent oxygen loss during sintering at high temperatures. The extracted values of $R_g$ and $R_{gb}$ indicate that the La-doped CCTO ceramics are electrically heterogeneous, consisting of grains with small $R_g$ values separated by extremely large values of $R_{gb}$. Also, the highest $R_{gb}$ value among all the samples is shown for the ceramics with $x = 0.05$, which is consistent with its lowest $\tan\delta$ at low frequency. Hence, it is reasonable to conclude that high dielectric response of the $Ca_{1-x}LaxCu_3Ti_4O_{12}$ ceramics originates from the Internal Barrier Layer Capacitance (IBLC) effect. The obtained $R_{gb}$ values can be correlated with temperature stability of $\varepsilon_r$. Low value of $R_{gb}$ of the pure CCTO may be the cause for its poor temperature stability whereas the La-doped CCTO ceramics, owing to their high $R_{gb}$ values, exhibit excellent temperature stability with reduced dielectric loss.

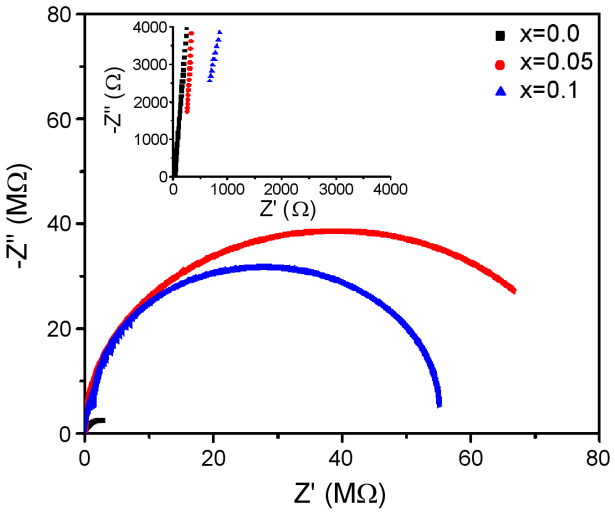


**Figure 8. Impedance complex plane plots ($Z^*$ plots) for $Ca_{1-x}La_xCu_3Ti_4O_{12}$ ceramics at RT; inset shows expanded view of high frequency tails close to the origin**

Figure 9 represents the frequency dependence of real ($Z'$) and imaginary part ($Z''$) of complex impedance ($Z^*$) of the $Ca_{1-x}La_xCu_3Ti_4O_{12}$ ceramics ($x = 0.05$) at some selected temperatures. It is clear from Fig. 9a that magnitudes of $Z'$ gradually decrease with increasing frequency and temperature at low frequencies followed by merging of curves into one at higher frequencies indicating the possible release of space charge [32]. This trend is a clear indication of increase in conductivity of the material with increasing temperatures and frequencies, which is in good accord with the AC conductivity results discussed above.

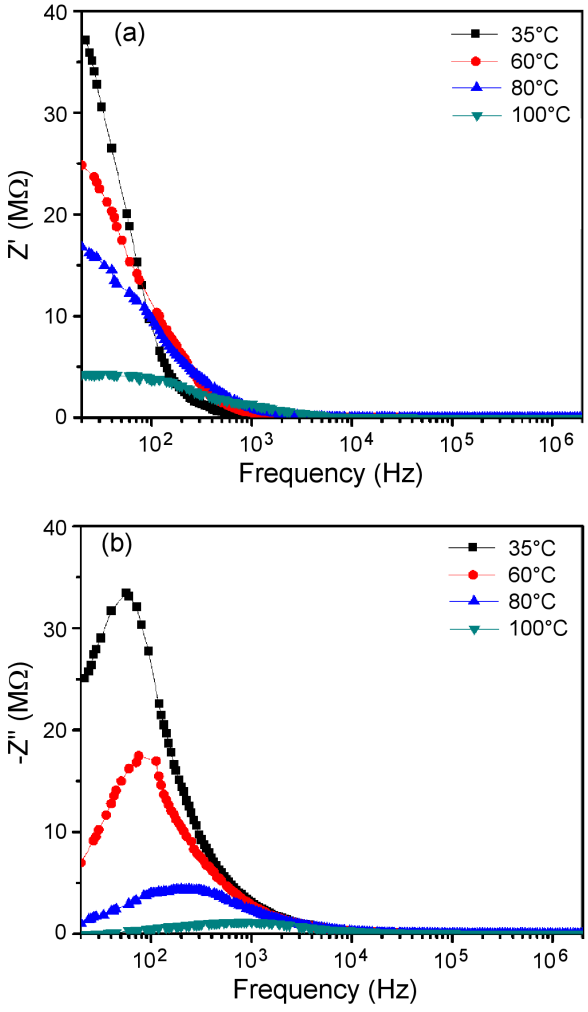


**Figure 9. Frequency dependence of (a) real ($Z'$) and (b) imaginary part ($Z''$) of complex impedance ($Z^*$) of $Ca_{1-x}La_xCu_3Ti_4O_{12}$ ceramics ($x = 0.05$) at some selected temperatures**

The suppression and shift of relaxation peaks ($Z''$) with increase in temperature along with merging of curves at high frequency for all the temperatures is clearly observed in Fig. 9b. This is a clear sign of possible release of space charge at grain boundaries together with the presence of a temperature-dependent dielectric relaxation process in the material [33]. The existence

of immobile species or electrons at low temperature and defects or vacancies at high temperatures [34] is responsible for such relaxation process. In addition, asymmetrical broadening of relaxation peaks with rising temperature suggests a distribution of relaxation time involved in the relaxation process.

## IV. Conclusions

In conclusion, lanthanum doping in giant dielectric material CCTO has been done through molten salt route of eutectic mixture within only one-hour (1 h) reaction time. X-ray powder diffraction analysis carried out on calcined powders confirms the formation of monophasic compounds up to $x = 0.1$ La substitution. The microstructure analyses reveal that the mean grain size is significantly reduced by La substitution which has the ability to inhibit grain growth thereby causing a reduction in the values of $\varepsilon_r$ and $\tan\delta$. Frequency and temperature dependent dielectric spectra validate that the La-doped CCTO ceramics ($x = 0.05$) developed via this route shows great promise for dielectric loss management ($\tan\delta < 0.03$ in the frequency range from 5 to 120 kHz at room temperature). Further, it shows nearly frequency independent dielectric constant ($\varepsilon_r > 2200$) from 1 kHz to 1 MHz and negligible variation in $\varepsilon_r$ with temperature at high frequency (typically $\Delta\varepsilon_r < 15\%$ at 10 kHz) in the temperature range of 30–140 °C. Based on the above-mentioned results, it can be concluded that facile molten salt is an efficient synthesis method to improve the dielectric properties of La-doped CCTO with very low dielectric loss and reasonable dielectric constant which are competitive with previous reports and make them a favourable contender for miniaturized capacitor application.

**Acknowledgements:** The author gratefully acknowledges Dr. K.K. Chattopadhyay, Professor, Department of Physics, Jadavpur University and Dr. Ramaprasad Maiti, Assistant Professor, Department of Electronics, Dirozio Memorial College, Kolkata for providing FE-SEM analysis and dielectric measurement facility, respectively

## References

1. M.A. Subramanian, D. Li, N. Duan, B.A. Reisner, A.W. Sleight, "High dielectric constant in $ACu_3Ti_4O_{12}$ and $ACu_3Ti_3FeO_{12}$ phases", *J. Solid State Chem.*, **151** [2] (2000) 323–325.
2. D.C. Sinclair, T.B. Adams, F.D. Morrison, A.R. West, "$CaCu_3Ti_4O_{12}$: One-step internal barrier layer capacitor", *Appl. Phys. Lett.*, **80** [12] (2002) 2153–2155.
3. R. Lohnert, H. Bartsch, R. Schmidt, B. Capraro, J. Topfer, "Microstructure and electric properties of $CaCu_3Ti_4O_{12}$ multilayer capacitors", *J. Am. Ceram. Soc.*, **98** [1] (2015) 141–147.
4. P. Thiruramanathan, A. Marikani, S. Ravi, D. Madhavan, G.S. Hikku, "Fabrication of miniaturized high bandwidth dielectric resonator on patch (DRoP) antenna using high dielectric $CaCu_3Ti_4O_{12}$ nanoparticles", *J. Alloys Compd.*, **747** (2018) 1033–1042.
5. Y. Tian, X. Zhang, Y. Yang, Z. Liu, X. Huang, "Sol-gel synthesis and sensing study of perovskite $CaCu_3Ti_4O_{12}$ nanopowders", *Integr. Ferroelectr.*, **129** [1] (2011) 188–195.
6. A. Boontum, D. Phokharatkul, J.H. Hodak, A. Wisitsoraat, S.K. Hodak, "$H_2S$ sensing characteristics of Ni-doped $CaCu_3Ti_4O_{12}$ films synthesized by a sol-gel method", *Sens. Actuators B Chem.*, **260** (2018) 877–887.
7. S. Maity, M. Samanta, A. Sen, K.K. Chattopadhyay, "Investigation of electrochemical performances of ceramic oxide $CaCu_3Ti_4O_{12}$ nanostructures", *J. Solid State Chem.*, **269** (2019) 600–607.
8. R.K. Pandey, W.A. Stapleton, J. Tate, A.K. Bandyopadhyay, I. Sutanto, S. Sprissler, S. Lin, "Applications of CCTO supercapacitor in energy storage and electronics", *AIP Adv.*, **3** [6] (2013) 062126.
9. M. Sahu, S. Hajra, R.N.P. Choudhary, "Structural, electrical and dielectric characteristics of strontium-modified $CaCu_3Ti_4O_{12}$", *SN Appl. Sci.*, **1** (2019) 13.
10. F. Gaâbel, M. Khlifi, N. Hamdaoui, L. Beji, K. Taibi, J. Dhahri, "Microstructural, structural and dielectric analysis of Ni-doped $CaCu_3Ti_4O_{12}$ ceramic with low dielectric loss", *J. Mater. Sci. Mater. Electron.*, **30** (2019) 14823–14833.
11. E. Swatsitang, K. Prompa, T. Putjuso, "Very high thermal stability with excellent dielectric, and non-ohmics properties of Mg-doped $CaCu_3Ti_4O_{12}$ ceramics", *J. Mater. Sci. Mater. Electron.*, **29** (2018) 12639–12651.
12. J. Boonlakhorn, P. Thongbai, "Dielectric properties, nonlinear electrical response and microstructural evolution of $CaCu_3Ti_{4-x}Sn_xO_{12}$ ceramics prepared by a double ball-milling process", *Ceram. Int.*, **46** [4] (2020) 4952–4958.
13. J. Jumpatam, B. Putasaeng, N. Chanlek, P. Kidkhunthod, P. Thongbai, S. Maensirie, P. Chindaprasir, "Improved giant dielectric properties of $CaCu_3Ti_4O_{12}$ via simultaneously tuning the electrical properties of grains and grain boundaries by $F^-$ substitution", *RSC Adv.*, **7** (2017) 4092–4101.
14. R. Espinoza-Gonzáleza, S. Hevia, A. Adrian, "Effects of strontium/lanthanum co-doping on the dielectric properties of $CaCu_3Ti_4O_{12}$ prepared by reactive sintering", *Ceram. Int.*, **44** [13] (2018) 15588–15595.
15. J. Boonlakhorn, P. Kidkhunthod, P. Thongbai, "A novel approach to achieve high dielectric permittivity and low loss tangent in $CaCu_3Ti_4O_{12}$ ceramics by co-doping with $Sm^{3+}$ and $Mg^{2+}$ ions", *J. Eur. Ceram. Soc.*, **35** [13] (2015) 3521–3528.
16. M.M. Shahraki, H. Daeijavad, A.H. Emami, M. Abdollahi, A.H. Karimi, "An engineering design based on nano/micro-sized composite for $CaTiO_3/CaCu_3Ti_4O_{12}$ materials and its dielectric and non-ohmic properties", *Ceram. Int.*, **45** (2019) 21676–21683.
17. W. Makcharoen, T. Tunkasir, "Microstructures and dielectric relaxation behaviors of pure and tellurium doped $CaCu_3Ti_4O_{12}$ ceramics prepared via vibro-milling method", *Ceram. Int.*, **39** (2013) S359–S364.
18. R. Espinoza-González, E. Mosquera, "Influence of micro and nano particles of zirconium oxides on the dielectric properties of $CaCu_3Ti_4O_{12}$", *Ceram. Int.*, **43** [17] (2017) 14659–14665.
19. L. Feng, X. Tang, Y. Yan, X. Chen, Z. Jiao, G. Cao, "Decrease of dielectric loss in $CaCu_3Ti_4O_{12}$ ceramics by La

doping", *J. Phys. Stat. Sol. A*, **203** [4] (2006) R22–R24.
20. S. Vangchangyia, T. Yamwong, E. Swatsitang, P. Thongbai, S. Maensiri, "Selectivity of doping ions to effectively improve dielectric and non-ohmic properties of $CaCu_3Ti_4O_{12}$ ceramics", *Ceram. Int.*, **39** [7] (2013) 8133–8139.
21. S. Jin, H. Xia, Y. Zhang, "Effect of La-doping on the properties of $CaCu_3Ti_4O_{12}$ dielectric ceramics", *Ceram. Int.*, **35** [1] (2009) 309–313.
22. P. Cheng, Z. Cao, M. Zhou, Q. Wang, S. Li, J. Li, "Dielectric properties of $CaCu_3Ti_4O_{12}$ ceramics doped by $La^{3+}$", *Ceram. Int.*, **45** [12] (2019) 15320–15326.
23. X. Huang, H. Zhang, J. Li, Y. Lai, "Influence of different dopant sites by lanthanum on the dielectric properties of $CaCu_3Ti_4O_{12}$ ceramics", *J. Mater. Sci. Mater. Electron.*, **27** (2016) 11241–11247.
24. A. Srivastava, O. Parkash, D. Kumar, P. Maiti, "Structural and dielectric properties of lanthanum doped $CaCu_3Ti_4O_{12}$ for capacitor application", *Am. J. Mater. Synth. Process.*, **2** [6] (2017) 90–93.
25. R.D. Shannon, "Revised effective ionic radii and systematic studies of inter atomic distances in halides and chaleogenides", *Acta Cryst.*, **A32** (1976) 751–767.
26. B.S. Prakash, K.B.R. Varma, "Influence of sintering conditions and doping on the dielectric relaxation originating from the surface layer effects in $CaCu_3Ti_4O_{12}$ ceramics", *J. Phys. Chem. Solids*, **68** [4] (2007) 490–502.
27. P. Lunkenheimer, S. Krohns. S. Riegg, S.G. Ebbinghaus, A. Reller, A. Loidl, "Colossal dielectric constants in transition-metal oxides", *Eur. Phy. J. Spec. Top.*, **180** (2009) 61–89.
28. J. Wu, C.W. Nan, Y. Lin, Y. Deng, "Giant dielectric permittivity observed in Li and Ti doped NiO", *Phys. Rev. Lett.*, **89** [21] (2002) 217601.
29. Y. Liu, W. Wang, J. Huang, F. Tang, C. Zhu, Y. Cao, "Dielectric properties of giant permittivity $NaCu_3Ti_3NbO_{12}$ ceramics", *Ceram. Int.*, **39** [8] (2013) 9201–9206.
30. R. Schmidt, M.C. Stennett, N.C. Hyatt, J. Pokorny, J. Prado-Gonjal, M. Li, D.C. Sinclair, "Effects of sintering temperature on the internal barrier layer capacitor (IBLC) structure in $CaCu_3Ti_4O_{12}$ (CCTO) ceramics", *J. Eur. Ceram. Soc.*, **32** [12] (2012) 3313–3323.
31. A.R. West, T.B. Adams, F.D. Morrison, D.C. Sinclair, "Novel high capacitance materials: $BaTiO_3$:La and $CaCu_3Ti_4O_{12}$", *J. Eur. Ceram. Soc.*, **24** [6] (2004) 1439–1448.
32. L. Singh, I.W. Kim, W.S. Woo, B.C. Sin, H. Lee, Y. Lee, "A novel low cost non-aqueous chemical route for giant dielectric constant $CaCu_3Ti_4O_{12}$ ceramic", *Solid State Sci.*, **43** (2015) 35–45.
33. B. Behera, P. Nayak, R.N.P. Choudhary, "Impedance spectroscopy study of $NaBa_2V_5O_{15}$ ceramic", *J. Alloys Compd.*, **436** [1-2] (2007) 226–232.
34. C.K. Suman, K. Prasad, R.N.P. Choudhary, "Complex impedance studies on tungsten-bronze electroceramic: $Pb_2Bi_3LaTi_5O_{18}$", *J. Mater. Sci.*, **41** (2006) 369–375.